EFSUMB Course Book, 2nd Edition

Editor: Christoph F. Dietrich

Ultrasound of the prostate

Kathleen Möller[1], Friedrich Aigner[2], Christoph F. Dietrich[3]

[1]Medical Department I/Gastroenterology, SANA Hospital Lichtenberg, Berlin, Germany, [2]Department of Radiology - Medical University Innsbruck - Tirol Kliniken, [3]Kliniken Hirslanden Beau Site, Salem und Permanence, Bern, Switzerland;

Corresponding author:

Prof. Dr. Christoph F. Dietrich, MBA

Department Allgemeine Innere Medizin (DAIM), Kliniken Hirslanden Beau Site, Salem und Permanence, Bern, Switzerland

Tel.: (+) 41313357894. Email: c.f.dietrich@googlemail.com

Acknowledgment: Prof. Anthony Rudd for giving excellent advice.

Introduction

Assessment of the prostate by transabdominal ultrasound is most commonly performed as part of an abdominal assessment for sizing, in case of micturition symptoms, lower abdominal symptoms, urinary tract infections, urinary retention, renal insufficiency and urinary bladder catheter complications. In the case of dysuric complaints, residual urine can be determined in the urinary bladder.

The most common prostate diseases are inflammatory processes (prostatitis), hyperplasia and prostate carcinoma. Focal prostate lesions are cysts, calcifications, abscesses and benign prostate hyperplasia (BPH). Prostate carcinoma cannot usually be diagnosed by suprapubic transabdominal ultrasound.

High-resolution imaging of the prostate with visualisation of the detailed structures, the clarification of focal lesions and the diagnosis of prostate carcinoma is reserved for transrectal ultrasound (TRUS), magnet resonance imaging (MRI) and their multiparametric techniques (1). The detailed structures and the zonal anatomy are much better delineated in these procedures than in transabdominal ultrasound but even then are not always easy to differentiate. However, it is useful to know the details and anatomy of the normal prostate or changes visible on TRUS in order to assign any visible correlating changes on transabdominal ultrasound. In particular, understanding the zonal anatomy is important to better understand prostate changes and focal lesions. In this way, patients that are otherwise referred for TRUS and MRI can be diagnosed using TUS with good accuracy and several focal lesions be correctly classified.

Topographic remarks

The prostate is located caudal and dorsal to the urinary bladder. It is adjacent to the bottom of the trigone of the urinary bladder At the level of the cranial portions of the prostate, the seminal vesicles present dorsolateral and externally. These have a teardrop-shaped appearance, are hypoechoic and may have small non-echoic parts. Caudal and dorsal to the prostate, the rectum is visualized obliquely. The ventral rectal wall shows the typical five-layered structure. The visualization of the remaining rectal parts depends on its contents.

Figures 1-3 show the prostate gland in the male pelvis with reference to the surrounding organs (urinary bladder, seminal vesicle and rectum) [Figure 1 - 3].

Figure 1 **The transverse suprapubic section shows the urinary bladder (UB), the prostate (P) and the rectum (R) with the transducer directed caudally and dorsally.**

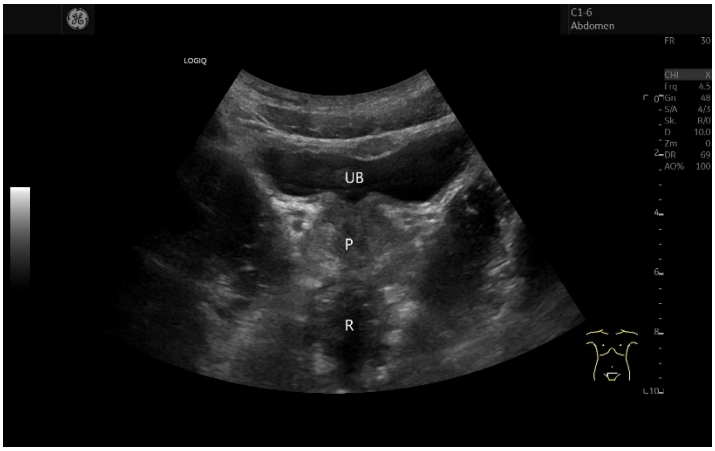

Figure 2 **The transverse section shows the seminal vesicles (SV) caudal to the urinary bladder (UB) and cranial and dorsolateral to the prostate. These are drop-shaped and their narrow side is directed towards the prostate or medially. The prostate is not visible in this plane.**

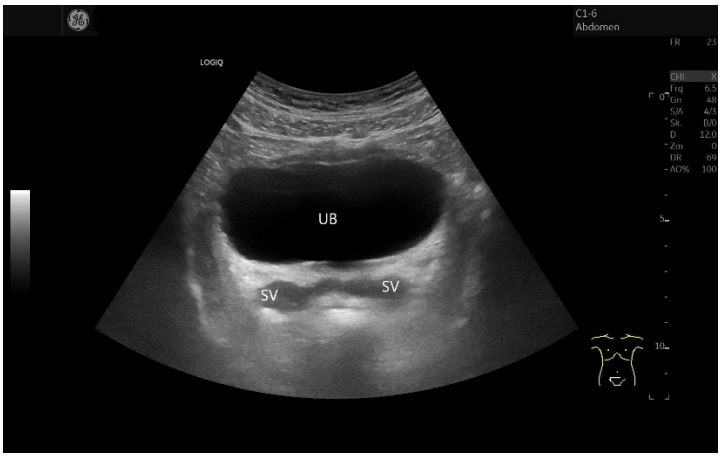

Figure 3 With a high-resolution transducer, here linear 9 MHz, it is sometimes possible to delineate the structure of the seminal vesicles (SV). Here, the liquid internal structures can be seen. Urinary bladder (UB); rectum (R).

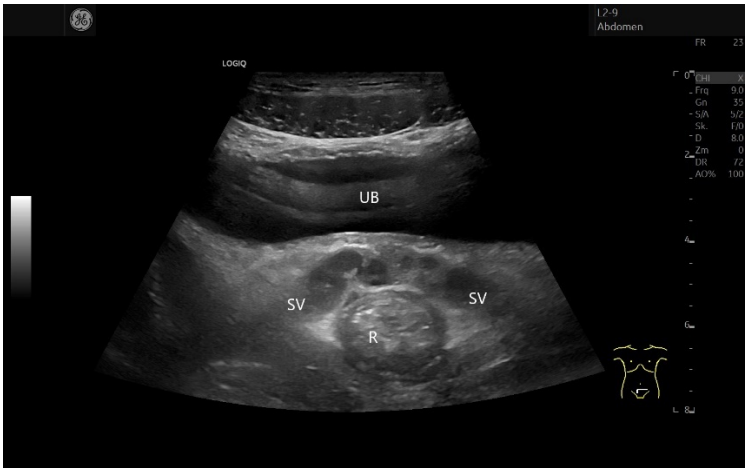

Anatomy

Anatomical orientation

The prostate has a chestnut or triangular shape. It has a smooth border. The base of the prostate is adjacent to the floor of the bladder. The apex faces the urogenital diaphragm. The urethra is located in the prostate gland. It consists of two segments: the proximal (near the urinary bladder) segment, also called the preprostatic segment, and the distal prostatic segment.

Parenchymal zones

The prostate is divided into several areas. Their visualization in transabdominal ultrasound is not possible in every patient. However, under good sonographic conditions and with higher resolution transducers, their delineation is possible in transabdominal ultrasound and not only transrectally. Even though the different zones are described mainly in transrectal ultrasound, it is useful to know them for abdominal ultrasound. Otherwise, the focal subdivided echogenicities could be misinterpreted when visible.

Current concepts of zonal anatomy are based on McNeal's autopsy studies (2). Four glandular zones are distinguished: ***Periurethral zone*** **(PUZ)*****, transitional zone*** **(TZ)*****, peripheral zone*** **(PZ)*****, central*** **zone (CZ)** and one stromal zone: ***anterior fibromuscular stroma*** **(AFS)** (3-6).

Periurethral zone*:* Central through the prostate runs the urethra. Behind the proximal prostatic urethra is the periurethral zone. This is hypoechoic, usually elongated tubular in configuration.

The periurethral glands are divided into two groups. The first are the superficial submucosally located glands in the proximal prostatic urethra. The second group is the deep group between the mucosa and inner longitudinal muscle layer emptying through long ducts into the urethra just above the verumontanum.

Transitional zone*:* Centrally located in the prostate is the transitional zone. The transitional zone surrounds the urethra near the verumontanum. In case of benign prostate hyperplasia (BPH) the TZ extends between the verumontanum and urinary bladder.

Verumontanum prostate (Caput gallinaginis or Colliculus seminalis) is an anatomical landmark. It is a mucosal fold on the posterior wall of the urethra with the orifice of the vas deferens with the vesicular gland and most of the excretory ducts of the prostate joining into the urethra.

The transitional zone contains many parts of musculature and connective tissue. It is hypoechoic and often nodular in configuration. The transitional zone is usually the site of origin of prostatic hyperplasia. The TZ increases with age (7). Prostate carcinoma rarely arises in this zone.

Peripheral zone*:* In the periphery of the prostate is the peripheral zone. This consists predominantly of glandular tissue. The peripheral zone is hyperechoic. Prostate carcinomas most often arise in the peripheral zone.

At the boundary between the TZ and PZ there is a band of fibromuscular tissue and compressed glandular tissue. This defines the TZ. In BPH, this band is strongly demarcated. In the literature, one encounters the term "surgical capsule".(5, 8).

Central zone*:* The central zone surrounds the ductus deferens and ejaculatory duct. The central zone has a conical teardrop shape. The tip of this cone points to the verumontanum on both sides. The verumontanum is located approximately in the middle of the prostatic urethra. The central zone is hypoechoic. Vas deferens, the ejaculatory duct and verumontanum are usually visible only on transrectal US.

Anterior fibromuscular stroma: The anterior fibromuscular stroma corresponds to a cap by which the prostate is fixed ventrally in the lesser pelvis. It is formed from striated smooth muscle. This is not visible on transabdominal ultrasound.

With age, the outer shape of the prostate changes. It becomes oval and ellipsoidal. This is caused by early BPH in the anteriorly located TZ. The anterior contour becomes expanded here. The posterior and lateral prostatic capsules are less elastic than the anterior fibromuscular stroma. There are therefore limits to the expansion of the transverse diameter, and for this reason the enlargement occurs predominantly in the anteroposterior diameter (3) [Figure 4 - 6].

Figure 4 **Here with linear transducer 9 MHz, the zonal anatomy is recognizable. The trigonum (T) of the urinary bladder is demarcated. The urethra runs centrally and the hypoechoic periurethral zone (PUZ) is visible centrally in the cranial parts of the prostate. The peripheral zone (PZ) on both sides is hyperechoic. In the lower third centrally, the verumontanum (V) is visible as an inhomogeneous structure. In the cranial part of the prostate laterally, the central zone (CZ) presents as a hyperechoic nodule with a punctiform ductus ejaculatorii (De).**

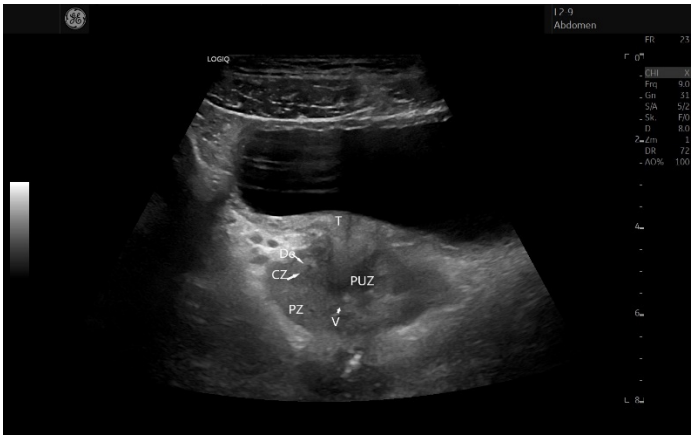

Figure 5 In the sagittal section, the ductus ejaculatorii (De) is shown longitudinally in the central zone (arrow mark). T Trigonum.

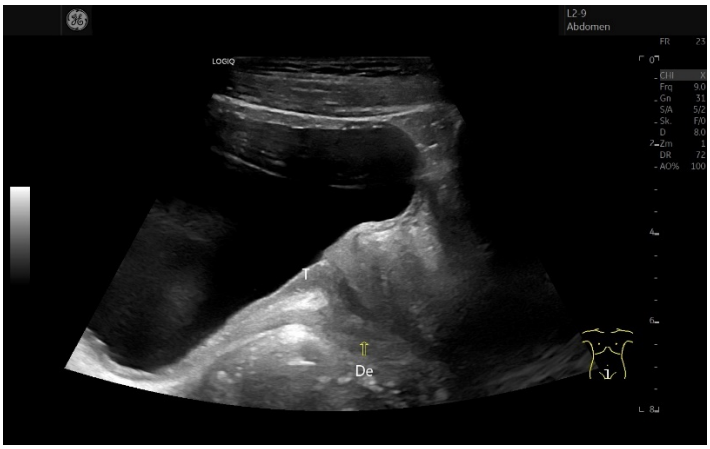

Figure 6 Normal zonal anatomy shows the periurethral zone (PUZ) and the peripheral zones (PZ). In the lower third centrally is the verumontanum (V).

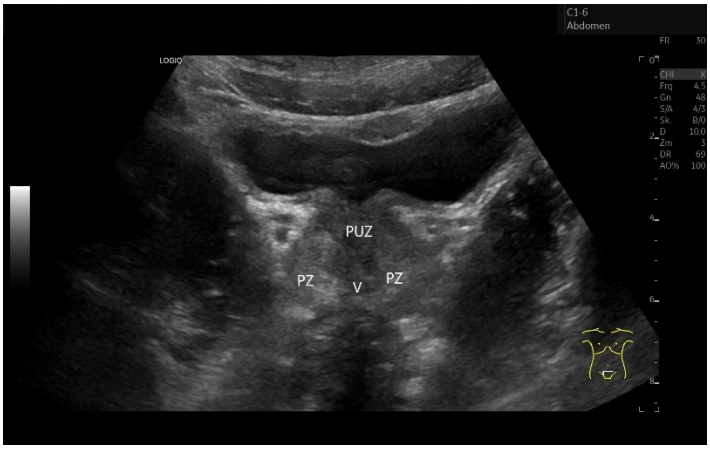

Transabdominal ultrasound examination technique

The percutaneous transabdominal ultrasound examination is performed with the abdominal sector transducer with frequencies of 2 - 6 MHZ. In very slim patients, the linear transducer with frequencies up to 9 MHz can also be used in some cases.

The examination of the prostate is performed ideally with a filled urinary bladder but is also possible with different filling status of the urinary bladder. The filled urinary bladder provides a good acoustic window. At the same time, associated changes such as a barred bladder due to prostatic hyperplasia and urethral obstruction can be delineated.

The patient is in the supine position. The transabdominal examination is performed with suprapubic transducer position in cross-section and longitudinal section. The transducer is directed caudally and dorsally.

When assessing the prostate, the shape, contour and symmetry are evaluated. Attention is paid to focal hypoechoic lesions, other focal lesions such as cysts and calcification. The sagittal transducer position can be used to assess whether there is protrusion of a hypertrophied middle lobe into the urinary bladder lumen.

To determine size and volume, the width is measured in cross-section and the height and length in longitudinal section (9). The height can also be measured in transversal section.

The assessment of the prostate also includes the examination of neighboring organs such as the urinary bladder and seminal vesicles and the assessment of regional, lymph nodes. Such as the parailiac nodes [Figure 7].

Figure 7 The urinary bladder has multiple pseudodiverticula (a). The cause is hyperplasia of the prostate. In the sagittal section, an enlarged part of the prostate (arrow) protrudes into the lumen of the urinary bladder (b).

a

b

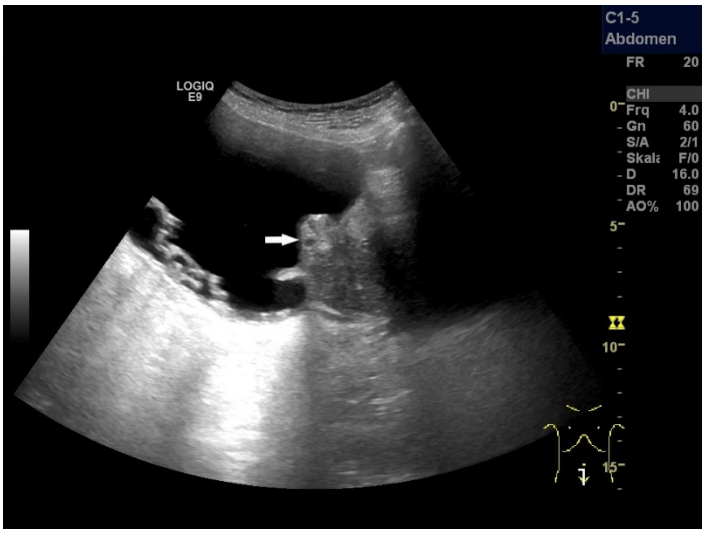

Transrectal ultrasound

Indications for transurethral ultrasound are pathological findings on rectal digital examination of the prostate, elevated PSA values, suspected prostate carcinoma, inflammatory changes, prostate abscess, surgical planning in benign prostatic hyperplasia and diagnosis of disorders of ejaculation. The volume measurement can be done in B-TRUS. Furthermore, the displacement of the prostate in relation to the rectal wall, the seminal vesicles and the vas deferens can be assessed (6).

The rectal US is performed with electronic probes with a frequency of at least 8 MHz, better 10 MHz. The probes should have color Doppler imaging, including Power Doppler. For a multi-parametric TRUS, elastography and the possibility of contrast-enhanced low-MI TRUS are also required (10).

Size and volume

Sizing the prostate is performed in case of micturition problems and indications of urinary flow disorders. It can be done by measuring the diameters and determining the volume. There are numerous studies assessing the accuracy of transrectal, transabdominal, and transperineal ultrasound or 3D TRUS to calculate prostate volume (11-13). The volumes may be calculated as being slightly larger in the TRUS (11).

Width is measured in the transverse diameter. Length and height are measured in sagittal diameter (9). For height determination, it is advantageous to measure in sagittal section along the course of the urethra. The volume is calculated according to the formula of a rotational ellipsoid: Width x depth x length/ 0.52 [Figure 8].

Figure 8 **For volume determination, transverse diameter and height are measured in cross-section. The prostate is enlarged and hypoechoic. When looking closely, a narrow border of the hyperechoic peripheral zone is still visible at the lower edge of the picture, i.e., dorsally (arrow)(a). The length is determined in the sagittal section. The balloon of a urinary bladder catheter (arrow) is located in the lumen (b). The height can alternatively also be determined in the sagittal section (c).**

a

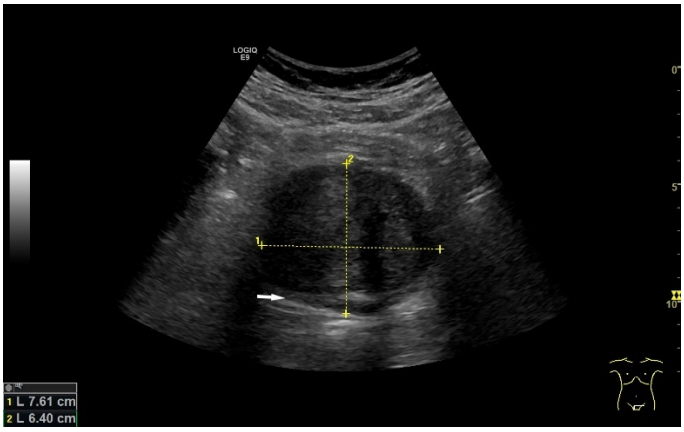

b

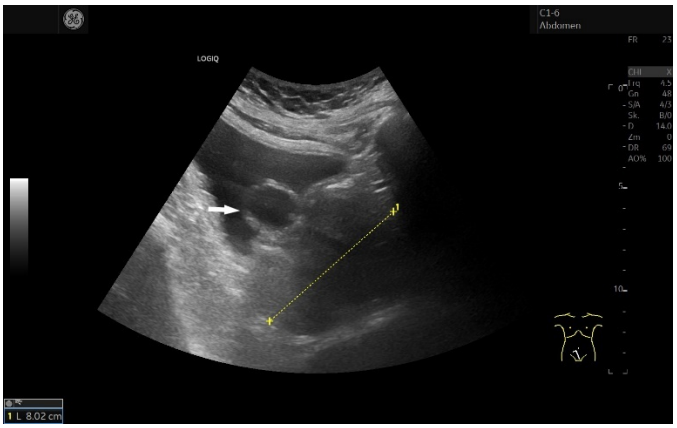

c

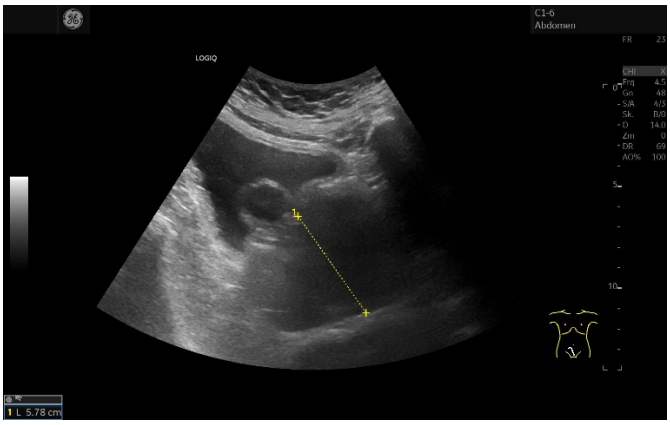

An enlarged prostate also changes its shape. The ellipsoidal shape becomes more spherical. And so there are suggestions that enlarged prostate volume should be calculated using the bullet formula with a coefficient of 0.66 rather than 0.52 (14) [Figure 9].

Figure 9 In an 18-year-old man, the prostate has the typical ellipsoidal shape (a). In a man over 80 years old it is round. This is caused by the hypoechoic hyperplastic parts, which lead to an enlargement of the organ and the circular shape (b).

a

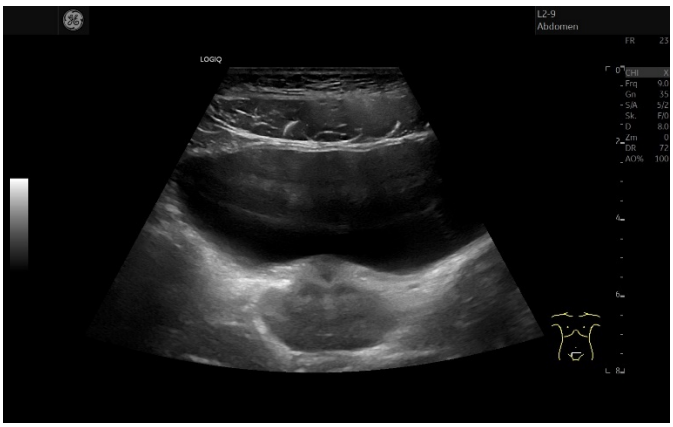

b

The volume calculation is performed either directly with corresponding calculation programs in the ultrasound unit or in the finding's documentation.

The standard values for abdominal ultrasound in adults are: 30 x 30 x 50 mm (15). The volume is < 15 m^3 before the hyperplasia develops (3). The normal volume is specified up to 25 m^3 (15) respectively 30-40 ml. Size and volume increase with age. In a Chinese study of men with lower urinary tract symptoms (LUTS), total prostate volume was 28.17+/-8.75 mm^3 in those aged 40-49; 30.83+/- 9.64 mm^3 in those 50-59 years old; and 35.036+/-17.41 mm^3 in those aged 60-70 (16).

Volume measurement can be performed in transabdominal ultrasound as well as in B-TRUS. Deviations of up to 10 % can occur in both procedures. The prolate spheroid formula W x W x H x pi /6 seems equally accurate and has the advantage of requiring measurements in the transversal plane only (15, 17). Enlargement appears in old age as a result of prostatic hyperplasia. Reduction occurs as a result of transurethral prostatic resection or after radiation. Ultrasound measurements can predict the natural history and progression of lower urinary tract symptoms and BPH and the therapeutic response to medical management.

The transitional zone increases with age. A special measurement is the determination of the ratio of the transitional zone volume (TZV) to the total volume of the prostate (TVP): Transitional zone Index (TZ index). This ratio correlates with symptom scores for lower urinary tract symptoms and with urodynamic measures of urine flow. This calculation is performed on TRUS (3, 7, 16). In the TRUS, the size of the transitional zone and the entire prostate are each measured in three dimensions, the respective volumes are calculated and then correlated (16).

Another option is to use the ratio of the anteroposterior diameter to the transverse diameter from TRUS. In the 5th decade of life, benign prostatic hyperplasia in the anterior TZ leads to a bulging of the anterior contour. The posterior and lateral prostatic capsule is less elastic than the anterior fibromuscular stroma. For this reason, the anteroposterior diameter increases in prostatic hyperplasia. Normal is a ratio of 0.5, values above 0.79 correspond to a pronounced hyperplasia. In transabdominal ultrasound, enlargement of the prostate with globular shape may correlate to this (3).

Seminal vesicles: In cases of drainage obstruction due to tumors, inflammation or hyperplasia, the seminal vesicles may swell and become enlarged. Anechoic areas may be visible.

Pathology

Hyperplasia

Benign prostatic hyperplasia (BPH) corresponds to growth of the glandular tissue and/or stromal tissue, in the latter also the muscle fibers. BPH can lead to enlargement of the prostate or parts of the prostate, obstruction and lower urinary tract symptoms (3, 18).

BPH is age-related (16). In men over 60 years of age, the prevalence of BPH is more than 50%, and in men over 85 it is as high as 90%. About 50% of men histologically diagnosed with BPH have moderate to severe lower urinary tract symptoms (LUTS) (3).

Benign prostatic hyperplasia develops in the central parts of the prostate - in the periurethral zone and transitional zone. But it is also present in the peripheral zone. The growth of the transition zone is the main factor in the overall growth of the prostate (16). This is especially true for the 50-69 age group (7, 16).

The first microscopic signs of hyperplasia arise in the periurethral glands posterior to the proximal urethra. Micronodular hyperplastic nodular changes then predominate in the transitional zone. Early visible ultrasound findings of BPH may be seen from the 4th decade of life onwards as symmetric, predominantly homogeneous hypoechoic round areas adjacent above and anterolateral to the region of the verumontanum (3).

As a result of hyperplasia, further hyperplastic nodular formation occurs in the transitional zone, and their fusion into larger nodular areas. Sonographically and on TRUS, predominantly hypoechoic changes present. In the course, diffuse heterogeneous or multinodular isoechoic

foci develop in the size-progressive transitional zone superimposed on a hypoechoic background. Hyperplasia may result in compression of fibromuscular stroma. This presents as a smooth hypoechoic band as a boundary of the hyperplastic adenomatous tissue and is also referred to as a "surgical" capsule (3). Atrophy of the peripheral zone is also possible (16).

Presumed lobus formation occurs and the hyperplastic periurethral glands develop into the **retrourethral (median) lobe**. In case of bladder neck herniation, the hyperplastic median lobe presents in the sagittal ultrasound transducer position as a presumed hypoechoic lesion protruding into the lumen of the urinary bladder. Knowledge of this change is important to differentiate it from polypoid bladder tumors.

Prostate volume (PV), transitional zone volume (TZV), transitional zone index (TZI), and intravesical prostatic protrusion (IPP) were all positively associated with BPH progression (18). The volume is important for treatment planning in case of corresponding symptoms and confirmed indication (3, 14). Most surgeons consider prostatic volume greater than 75 cm^3 an indication for open resection and favor TURP when the volume is less than 75 cm^3. When the prostate has a volume of less than 30 cm^3, especially in younger men, a transurethral incision of the prostate (TUIP) can be performed. For interventions with radiofrequency transurethral needle ablation, a limit of 60 cm^3 is recommended. Therapy with 5a-reductase inhibitors are less effective on obstruction in prostate volume less than 50m^3. (3). Size and volume are determined as part of the therapy control for BPH.

Neil F Wasserman described a classification of benign prostatic hyperplasia for ultrasound (3). This is based on Randall's classification (19). This ultrasound classification refers to transurethral ultrasound but is applicable to transabdominal US [See Table 1].

The different variants of hyperplasia are shown schematically in sagittal section for better understanding. The illustrations are based on those of N.F. Wasserman (3) [Figure 10 and 11].

Table 1 Classification of BPH for ultrasound application according to Wasserman (3).

Type	**Characteristic changes**
I	The transitional zone is hypoechoically enlarged on both sides. The urethra is displaced backwards.

II	Retrourethral hypoechoic enlargement. In the sagittal transducer position, a hypoechoic lesion bulges into the bladder and appears as a polypoid tumour. The tip of the hyperplasia is at the level of the verumontanum. With increasing enlargement, the urethra can be displaced anteriorly. In the optimal case, the urinary bladder wall is delineable. It is visible that the wall is lifted by the lesion and that the lesion is outside the bladder.
III	Hypoechoic enlargement of the transitional zones on both sides and of the retrourethral tissue.
IV	Hyperplasia of the periurethral tissue prolapses through the lumen of the urethra into the lumen of the bladder. "Pedunculated type". The tip of the hyperplasia is at the level of the verumontanum.
V	Hypoechoic enlargement of the transitional zone bilaterally and pedunculated hyperplasia of the periurethral tissue, which bulges over the lumen of the urethra into the urinary bladder. The tip of the hyperplasia is at the level of the verumontanum.
VI	Hypoechoic hyperplastic focal lesion below the trigonum. Unlike retrourethral and pedunculated hyperplasia, there is a distance and no contact with the verumontanum. This hyperplasia is localised in the subtrigonal parts of the prostate. There is no tip at the level of the verumontanum.

Figure 10 **Sagittal section of prostate without hyperplasia. UB-Urinary bladder, PUZ-periurethral zone, TZ-transitional zone, U-Urethra, CZ-central zone, PZ-peripheral zone, SV-seminal vesicle.**

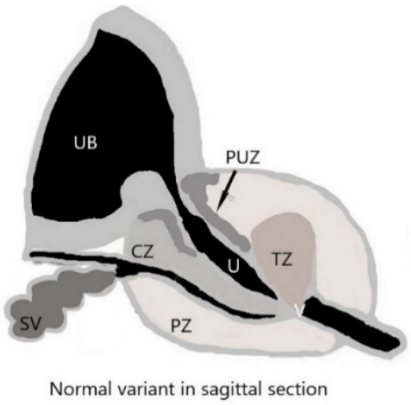

Figure 11 **Different localizations of prostate hyperplasia according to the classification of N.F. Wasserman (3). Sagittal section of prostate. TZ-transitional zone, RU-retrourethral, PH-pedunculated hyperplasia, H- hyperplasia.**

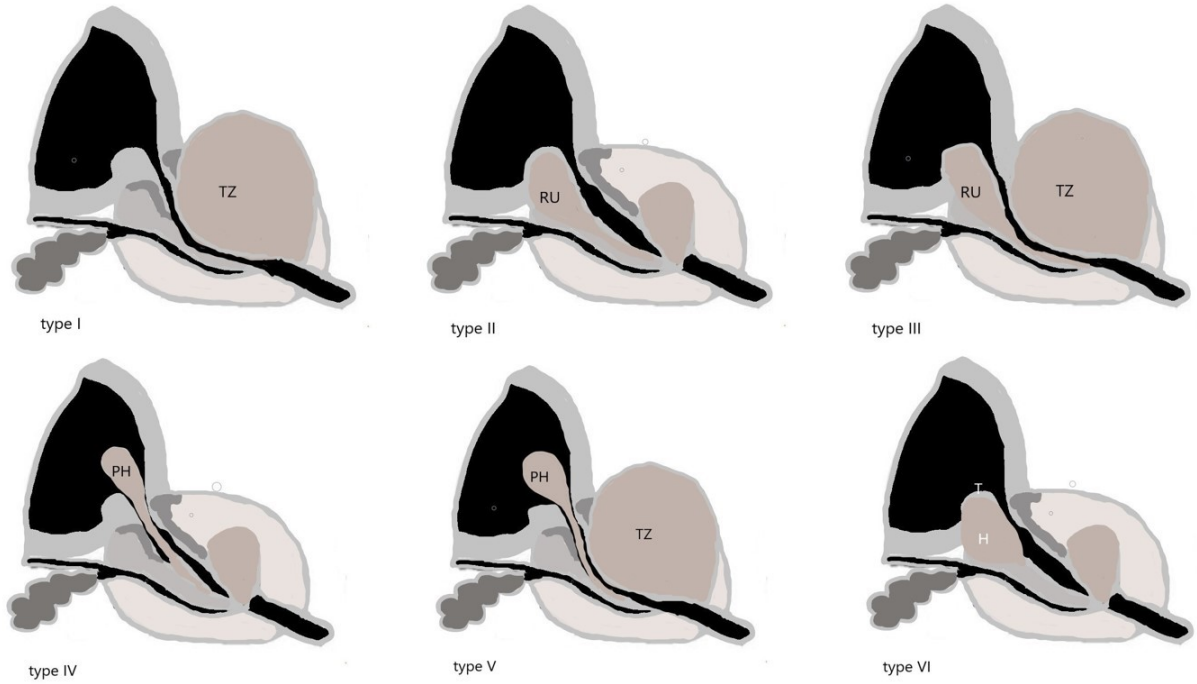

BPH - what is clearly visible in transabdominal ultrasound?

In cross-section: the enlargement of the periurethral hypoechoic zone and the hypoechoic enlargement of the transitional zone with narrowing of the peripheral zone.

In the sagittal section: hyperplastic portions protruding into the lumen are visible. Whether these are hyperplasia of the periurethral zone or pedunculated parts prolapsing into the lumen cannot be differentiated on ultrasound [Figure 12 - 15].

Figure 12 Prostate in cross section. Hypoechoic enlargement of the TZ on both sides. The bottom of the urinary bladder is distended. The peripheral zone is narrowly recognizable in the dorsal area. The border area between the TZ and PZ is marked with an arrow.

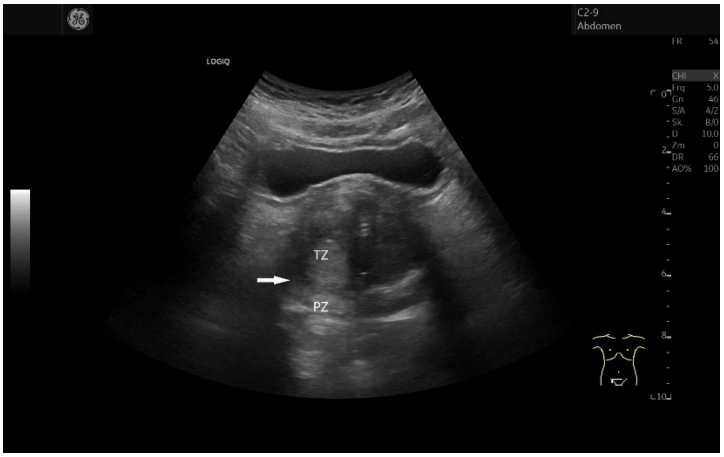

Figure 13 Hypoechoic enlarged and rounded prostate in cross-section with enlarged TZ. The PZ is narrow (a). In sagittal section it is visible that the urethra is displaced (white arrow). A hyperechoic nodule (yellow arrow) is visible at the base of the urinary bladder (b). This corresponded to a thickening of the trigone of the urinary bladder in transversal section (c) and in the MRI.

a

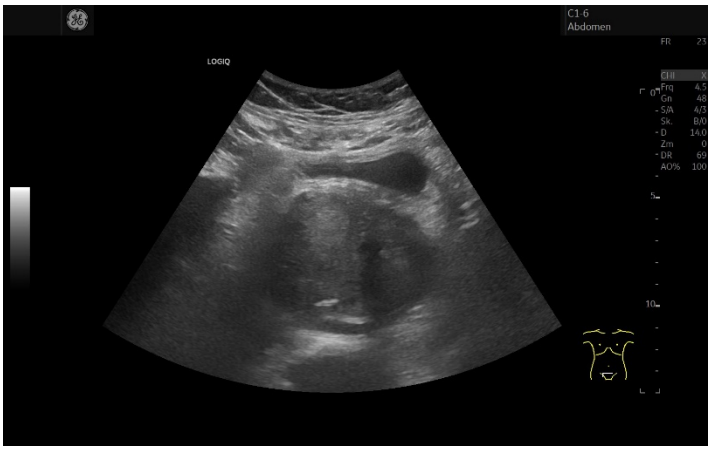

b

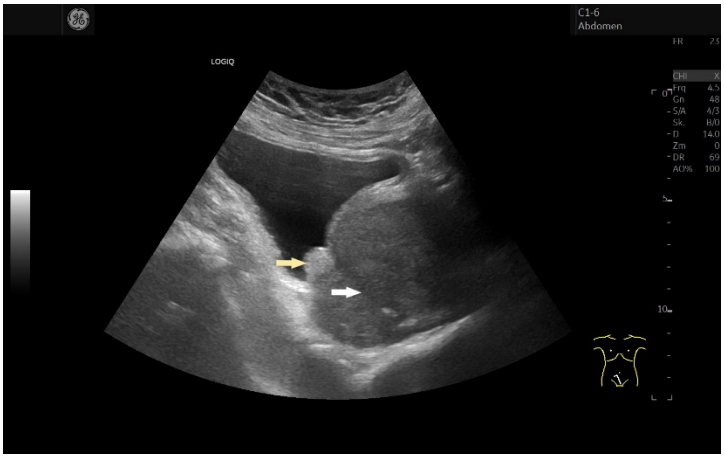

c

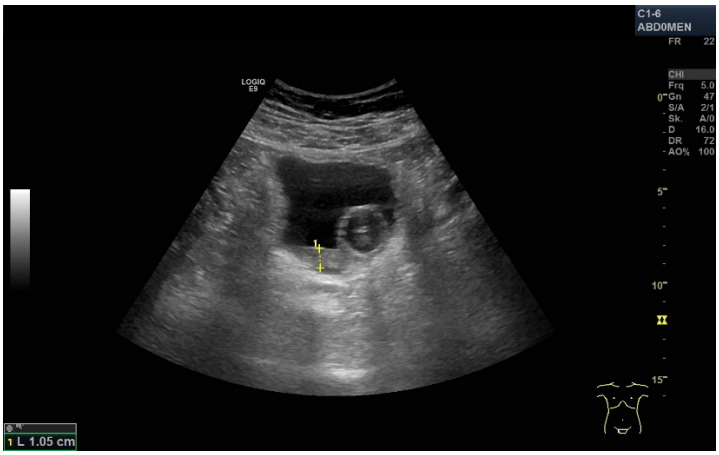

Figure 14 In cross-section, the periurethral zone is enlarged on both sides of the urethra (arrow). In this hypoechoic hyperplasia there is a cyst and a calcification (a). In

the sagittal section, hyperplastic portions are protruding into the lumen of the urinary bladder. A small cyst presents in this cone (b).

a

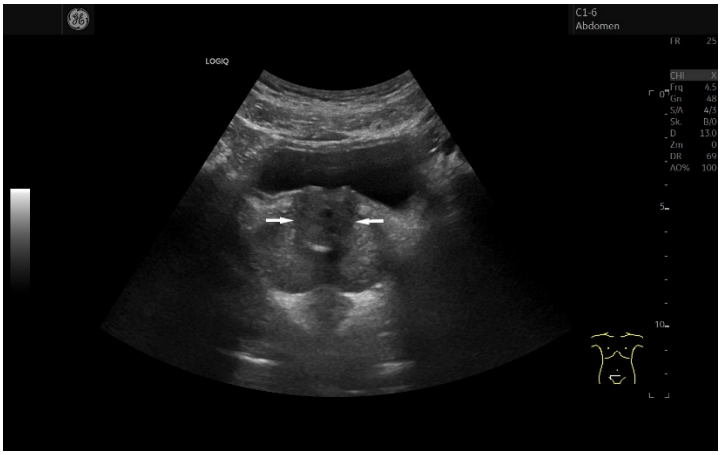

b

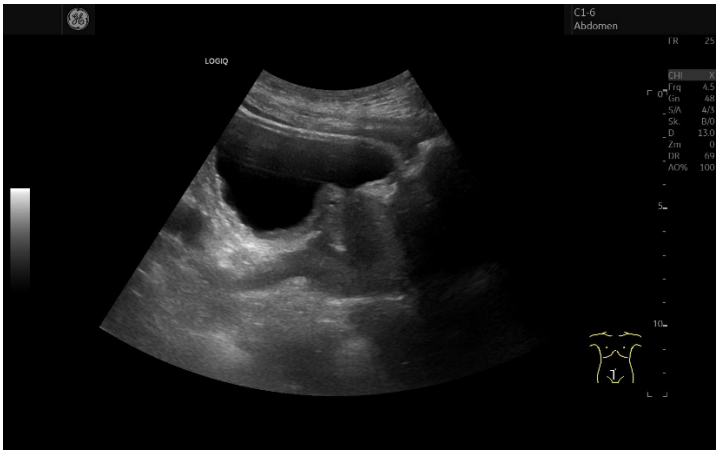

Figure 15 In cross-section, hypoechoic changes are visible in the enlarged TZ on both sides (a). In the sagittal section, hyperplastic parts of the prostate bulge into the lumen of the urinary bladder (b).

a

b

Cysts

Cysts of the prostate are related to atrophy of the prostate gland as well as to inflammatory disease, benign prostatic hyperplasia, ejaculatory duct obstruction and cancer (20). Most of the time, prostate cysts are incidental findings and harmless, without clinical significance. However, they should always be seen in the overall context. In transabdominal ultrasound it is not possible to differentiate and assign the small parenchymal cysts or duct ectasia. Knowledge of the genesis and that these are usually harmless findings is nevertheless useful. The cystic lesions show the typical cyst criteria with delicate smooth border, entry echo, exit echo, nonechoic lumen, dorsal sound enhancement and tangential cyst margin shadow.

- *Prostatic urethra cysts, formerly cyst of the Müllerian duct:* small cysts in the prostate in the median dorsal and cranial sections, in the midline above the level of the

verumontanum and between the seminal vesicles correspond to utricle cysts. These are residues of the embryonic Müller duct. These are harmless. Differentially, it may still be a ureteral ectopia (8, 20).

- *Cystic dilatation of the prostatic urethra or cystic utricle*: these cysts develop at later stages after the utricle is completely formed and they are probably due to obstruction of the communication through the urethra (20).
- *Enlarged prostatic urethra:* This is not a real cyst. Children or young adults are affected, usually other malformations are present (20).
- *Cysts of the ejaculatory duct*. These are congenital or acquired. They are located above the level of the verumontanum. They can be unilateral or bilateral (20).
- *Parenchymal cysts*: They are acquired due to the retention of prostatic secretions. These are multiple thin cysts. Causes are difficult drainage of prostatic secretions, or obstruction of the ducts due to BPH nodules or inflammation. They are localized lateral, subcapsular or in the periurethral/bladder neck with asymmetrical growth (20) [Figure 16]. Ductal ectasia or microcysts can be related to the glandular retention of secretions or rarely to simple atrophy with cyst formation (SACF).
- *Complicated cysts due to hemorrhage or infection*: Due to interventions.
- *Cystadenoma and cystadenocarcinoma*: Large cystic-solid, septated masses (6).
- *Cysts in parasitic infections*: These are cysts in connection with bilharziasis (schistosomiasis) or hydatidosis (20).

Figure 16 Small cyst at the periphery subcapsular (arrow) (a). In figure (b), it is not a cyst but the filled balloon of a catheter balloon dislocated into the prostate.

a

b

Calcification

Calcification in the prostate is not uncommon and are seen especially in men over 40 years of age (21). Aging is correlated with the presence of calculi. They are frequently detected incidentally. Causes are infections, benign prostatic hyperplasia, but also carcinomas and radiation of prostate carcinoma. They may be present in chronic pelvic pain syndrome.

The precursors of the calcification are presumably corpora amylacea. These are small hyaline bodies. They develop from dead cells or thickened secretions. Analysis of the proteins in the corpora amylacea and the calculi of the prostate indicated that the predominant proteins in these calculi are proteins that participate in acute inflammation, particularly proteins contained in neutrophil granules (22). True prostatic stones arise from inflammation-induced

obstruction of the prostatic acini, then with stasis and retention of prostatic fluid along with desquamation of the acinar cells. This leads to the formation of corpora amylacea and the deposition of calcium salts (23).

According to their formation, prostate calcifications (PC) are often also categorized as endogenous PC and extrinsic PC. Endogenous PCs are mainly formed by prostatic secretions, while extrinsic PCs are caused by urine reflux and are often more extensive than endogenous PCs (24, 25). It appears that type I is caused by an obstruction of the prostatic secretions around a benign prostatic hyperplasia or as a result of chronic inflammation, and that type II PCs are associated with urinary reflux (24).

The detection of calcification in TRUS and CT is higher than in percutaneous ultrasound. Prostate calcification is commonly seen at the junction between the transition zone and peripheral zone against the background of BPH (5) [Figure 17]. However, they are also found in the region of the verumontanum and the ejaculatory canal [Figure 18]. Urethral stones are mostly located in the caudal part of the periurethral prostate tissue (23).

In ultrasound, they present as hyperechoic reflexes with dorsal sound cancellation. In transabdominal ultrasound, type A and type B can be classified (26). Type A are discrete small reflections in ultrasound. Type B are a large mass of multiple reflections. In analogy to ultrasound, in TRUS the prostatic calculi are divided into Type A (discrete small reflection) and Type B (large multi-reflective mass) (27). In X-rays, type I (a surface consisting of small spheres) and type II (a larger, multi-faceted surface) were described (28).

Most PC are asymptomatic. However, large or pronounced PC can be a significant risk factor for severe lower urinary tract symptoms (LUTS). It appears that patients with chronic prostatitis or chronic pelvic pain syndrome are more likely to have prostatic calculi and that these are associated with more intraprostatic inflammation (24, 29). Men with chronic bacterial prostatitis without prostatic calculi had a higher rate of continued microbiological eradication and a lower relapse rate (29). Calcification located in the peripheral zone can be an indication of prostate carcinoma (30).

Figure 17 At the junction between the transition zone and peripheral zone against the background of BPH there are calcifications (arrow).

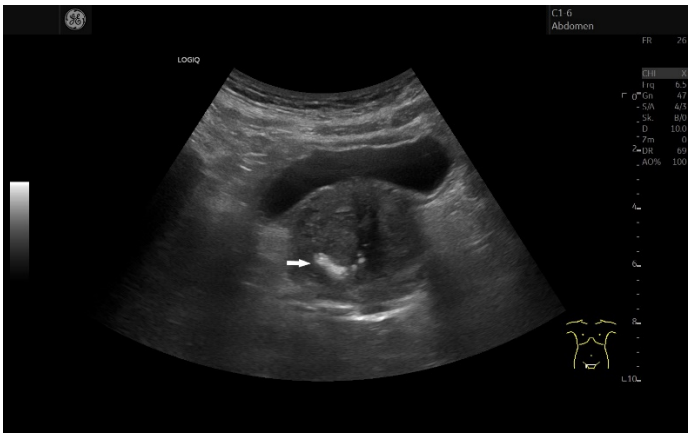

Figure 18 Calcifications occur centrally at the level of the verumontanum.

Prostatitis

Prostatitis is an inflammatory process in the prostate. It is divided into acute or chronic bacterial prostatitis, granulomatous prostatitis and IgG4-related prostatitis (31). Acute prostatitis has a two-tiered age distribution, affecting men between the ages of 20 to 40 years and men over 70 years (5). Causes for *bacterial* prostatitis include manipulation of the prostate, urethral stricture, benign prostatic hyperplasia (BPH), phimosis, urethritis, diabetes and other immunocompromising conditions. Infection most commonly occurs through intra-prostatic reflux of infected urine. The most common pathogens are Escherichia coli, but also

other Gram-negative organisms such as Klebsiella, Proteus and Pseudomonas, as well as Gram-positive Enterococcus species (31).

Acute prostatitis manifests with dysuric complaints, pulling, burning and pain in the anorectal area, but also systemic signs of infection. Chronic prostatitis exists when the prostate infection lasts longer than 3 months. Bacterial Prostatitis can be focal or diffuse involving both the PZ and TZ (5). A complication of bacterial prostatitis is prostate abscess (5, 31). *Granulomatous* prostatitis (GP) is an inflammatory disease characterized by the histological presence of epithelioid granulomas with or without other inflammatory cells. It arises because of previous mycobacterial or fungal infection, prostate biopsy, interventions at the prostate, transurethral prostate resection or systemic granulomatous infection (5, 31). Iatrogenic granulomatous prostatitis arises in connection with transurethral resection of the prostate or bladder because of a reaction to altered epithelium and stroma (8). Infectious granulomatous prostatitis may be caused by Mycobacterium tuberculosis, less commonly by Treponema pallidum, herpes zoster, and fungi (Cryptococcus, Candida, Aspergillus) (8). The involvement of the prostate in sarcoidosis has only been reported casuistically (32-34). One form of idiopathic granulomatous prostatitis is xanthogranulomatous prostatitis (31). Granulomatous prostatitis is rare and accounts for only about 1 % of all prostatitis. Clinically, granulomatous prostatitis may present as focal or diffuse induration that often feels rock-hard on rectal examination. The serum PSA level may be normal or elevated, hematuria may potentially be present (5). *IgG4 related prostatitis* is a relatively newly described manifestation (31, 35). Involvement of the genitourinary system in IgG4 related diseases (36) is rare and includes a variety of entities such as retroperitoneal fibrosis of the ureter or kidney, tubulointerstitial nephritis, pseudotumour of the bladder and hypovascular renal lesions. The clinical symptoms of IgG4-related prostatitis are similar to those of chronic prostatitis. Attention should be paid to other organ manifestations. For IgG4-associated diseases, the serum level of immunoglobulin G4 is 2-3 times higher (36).

Imaging of prostatitis is the domain of MRI. The most important MRI findings include focal or diffuse prostatic enlargement, T2 signal hypointensity, diffusion restriction and correspondingly low signal intensity on ADC maps (31).

What can be deduced using ultrasound?

In the case of severe diffuse prostatitis, the organ may be enlarged, have indistinct margins and be structurally disturbed. However, in many patients the structures are generally not delineated on transabdominal US. In addition to the described structural changes and more hypoechoic PZ, diffuse hypervascularization may be visible on TRUS. Acute bacterial prostatitis may show a hypoechoic rim around the prostate on US. hypoechoic rim around the prostate and colour Doppler show increased flow (15). *Abscesses* are hypoechoic and anechoic and may have a hyperechoic capsule (5) [Figure 19].

Figure 19 B-mode TRUS (a) shows a round, 5 mm hypoechoic lesion at the periphery of the prostate (arrow). On TRUS with CDI (b), this lesion (arrow) has no vessels. However, small vessels are visible at the periphery. Very small abscess in the context of prostatitis.

a

b

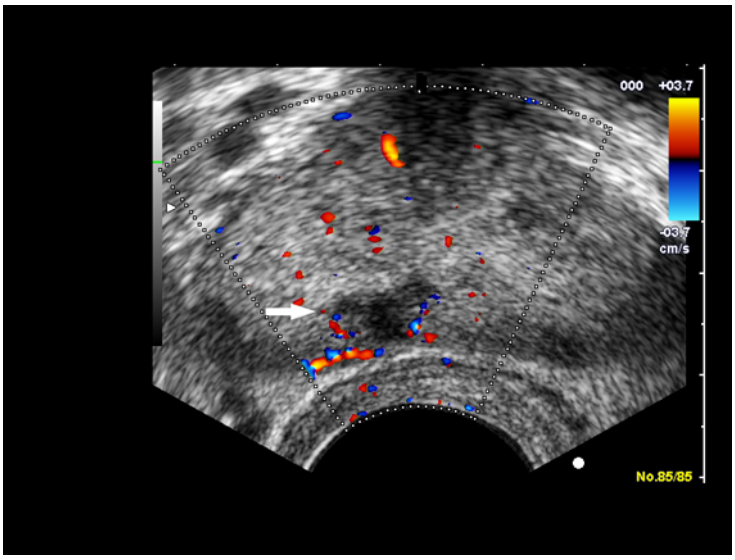

Postoperative changes

A common operation is transurethral prostatic resection (TURP). This shows a typical ultrasound image. The resection is mainly above the verumontanum so that the openings of the ejaculatory ducts are not injured or later obliterated with scarring. The resulting TURP defect seen on imaging is a typical wedge-shaped defect in the area of the prostate and bladder neck above the verumontanum [Figure 20].

Figure 20 After transurethral prostate resection, transabdominal ultrasound (a, b) and TRUS (c) show a typical wedge-shaped defect (markings and arrows).

a

b

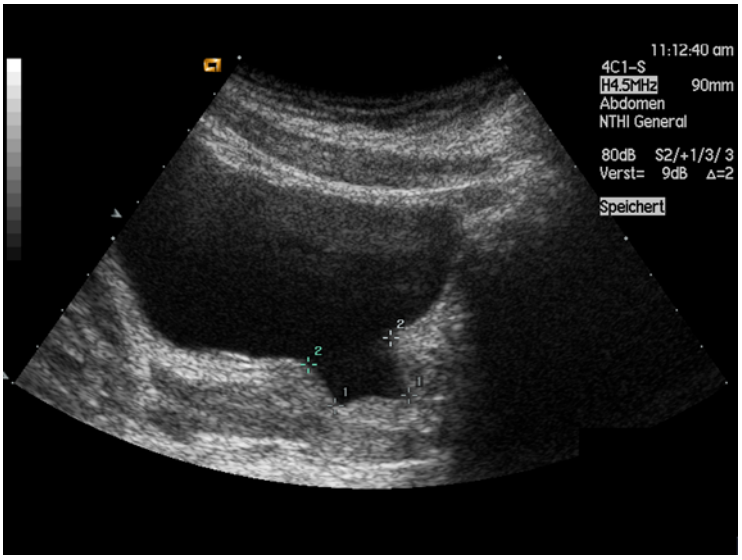

c

Prostate carcinoma

The diagnosis of prostate carcinoma is not usually made by abdominal ultrasound. Only in the case of extensive tumors that require space and cross contours can US be diagnostic [Figure 21 and 22]. This also applies to the rare sarcoma [Figure 23].

Figure 21 **Enlarged hypoechoic altered prostate with ill-defined external contours. The latter are mainly suspect in transabdominal ultrasound for carcinoma. Advanced metastatic prostate carcinoma was known in this patient.**

Figure 22 **Irregular polycyclic limited hypoechoic changes exceeding the contour and capsule of the prostate in a known prostate carcinoma.**

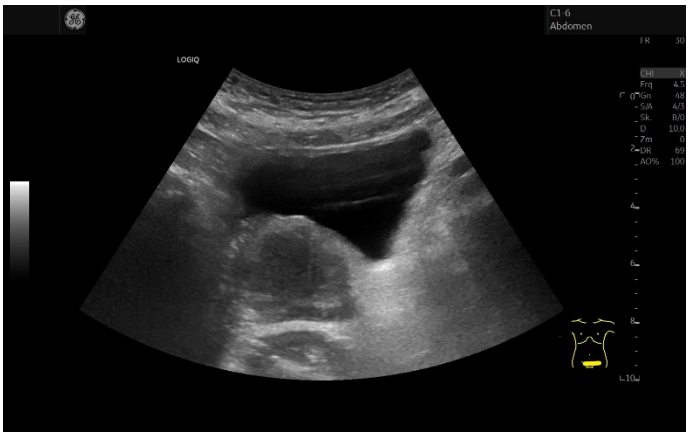

Figure 23 **A very large hypoechoic mass presents in the prostate area (a, b) (marking). The normal prostate is not delineated. The urinary bladder here is barely filled. From the sonomorphological aspect it is a large tumor, histologically in this case a sarcoma.**

a

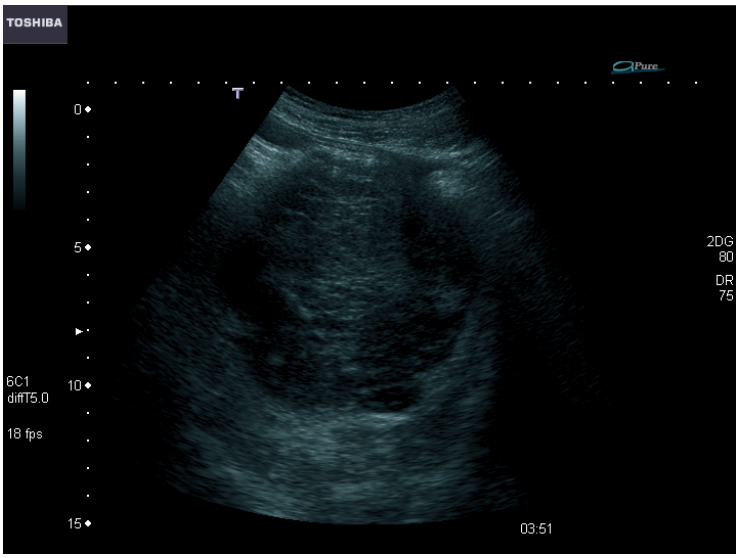

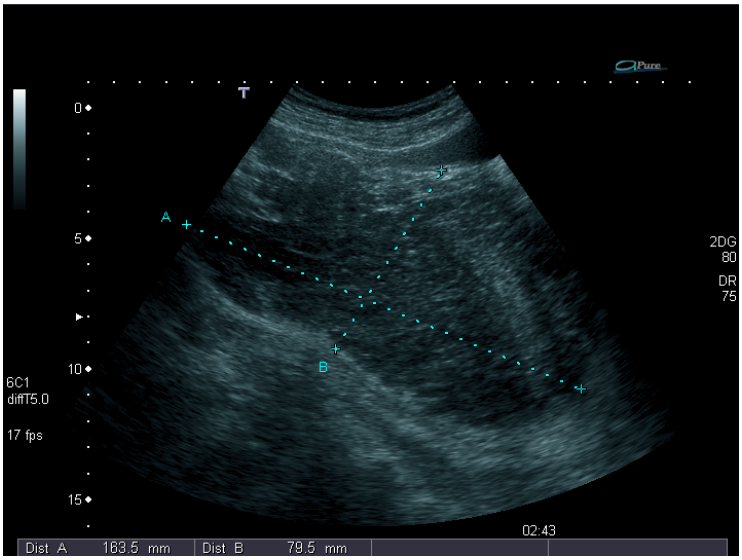

Multiparametric MRI is considered the standard diagnostic method for prostate carcinoma. In specialized centers, modern (multiparametric) TRUS procedures are also used to increase the detection rate of significant carcinomas (10, 37, 38). TRUS is used to assess tissue morphology using B-mode morphology. 70% of prostate carcinomas develop in the peripheral zone. Only 20 % originate from the transitional zone and 10 % from the central zone (15). In TZ, there is the difficult task of distinguishing carcinoma from hyperplasia. On B-mode TRUS the carcinoma may be hypoechoic, but also isoechoic. TRUS is limited in particular in tumor detection in the TZ, CZ and in the far anterior parts/ AFS, especially in the case of enlarged prostate. The typical prostate carcinoma of the peripheral zone is described as hypoechoic

and nodular in the B-TRUS and is elastographically stiffer. Vascularization is asymmetrically increased in the area of the carcinoma; the normal radial structure is abolished. In Contrast enhanced (CE-TRUS), rapid enhancement and rapid washout are tumor-suspicious (4). Using CE-TRUS, the diagnosis of prostate cancer had an accuracy of 83% with a sensitivity and specificity of 90% and 78% respectively (38). Carcinoma in the TZ represents a special challenge for imaging. Due to hypertrophy occurring with age and inflammatory processes already present, these parts are often hard, hypervascular and diffusion disturbed. Structural imaging techniques are used here - T2-weighted MRI and B-TRUS. Appearances of carcinoma in the inner glandular sections on B-TRUS are hypoechoic, lentiform, linear, planar changes (4).

TRUS guided biopsy

The indications for TRUS biopsy of the Prostate are suspicious palpation findings and increased PSA. The TRUS-guided biopsy is carried out *systematically* in the B-mode TRUS or *targeted* in multiparametric (mp) imaging. The systematic US-guided prostate biopsy is performed according to the guidelines of the European Association of Urology (39, 40). The depiction of Prostate in B-mode served to delineate its various areas (sextant scheme). These are base, middle, apex, right and left. Two samples are taken here (4). ***Systematic*** biopsy is not sufficiently sensitive to detect the significant carcinomas. In TRUS guided biopsy, primarily the lateral and peripheral parts of the prostate are biopsied. Thus, up to 30% of significant carcinomas can escape biopsy (4, 41-43). In the ***targeted*** biopsy, samples are taken from areas that were conspicuous in the multiparametric MRI or TRUS imaging.

Multiparametric (mp) TRUS

The simultaneous use of structural and functional ultrasound techniques for the detection of prostate carcinomas is called multiparametric (mp) TRUS. The information from B-mode TRUS is combined with information about tissue properties (1, 4, 10). The mpTRUS is primarily used for the delineation and diagnosis of prostate carcinoma with identification of lesions for targeted biopsy. However, all other prostate diseases and focal lesions can also be imaged in the mpTRUS.

Elastography provides information about focal hardness properties. In the broadest sense, this is to supplement or optimize palpation in the deeper parts of the prostate that are not covered by the digital examination. The method used is strain elastography. It is important that the transducer points to the center of the prostate and is well coupled to the rectal wall. In the outer parts, it is true that a prostate carcinoma has a higher cell density compared to healthy tissue and is therefore stiffer (1, 15, 44) [Figure 24]. In the inner parts of the prostate, the specificity is unfortunately quite limited, because with increasing age and enlargement of the prostate, it also becomes harder. Focal inflammatory areas and hyperplastic nodules may also be harder and thus feign false positive findings of prostate carcinoma. The sole benefit of elastography is therefore limited.

Figure 24 Large hypoechoic lesion in the marginal areas of the prostate (arrows), in elastography stiffer (arrows) than the rest of the prostate. In this case prostate carcinoma.

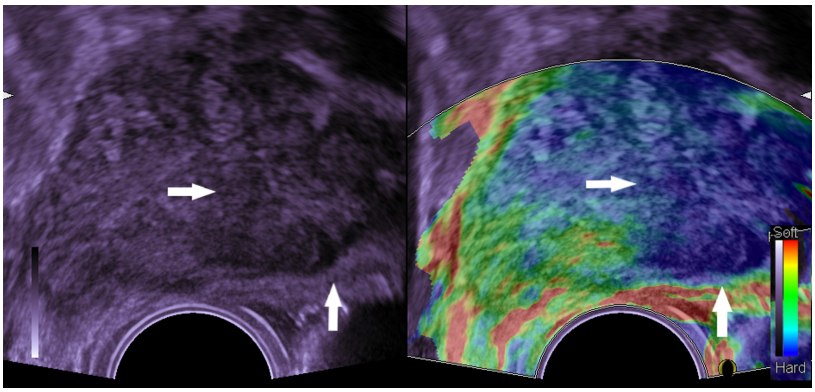

Color Doppler imaging TRUS demonstrates blood flow in macrovessels, vascular architecture and focal features of vascularization (1). The flow velocities are set very low at max. 5 cm/sec. The colour gain is maximized so that no artefacts appear. The outer parts of the prostate are hypovascular compared to the inner parts and show a radial macrovascular pattern (4, 15). Microvascular density is high in prostate cancer. With the aid of color Doppler imaging, tumor angiogenesis can be visualized [Figure 25]. The disadvantage is that inflammatory lesions or hyperplastic areas also show increased vascularization. The inner parts of the prostate are already more vascularized (4, 10).

Figure 25 Prostate after TURP with wedge-shaped defect of the prostate on TRUS. The prostate is very inhomogeneous in hyperplasia. CE CDI TRUS shows a hypervascularised area at the periphery of prostate(arrow). In further diagnostics, this corresponded to a carcinoma.

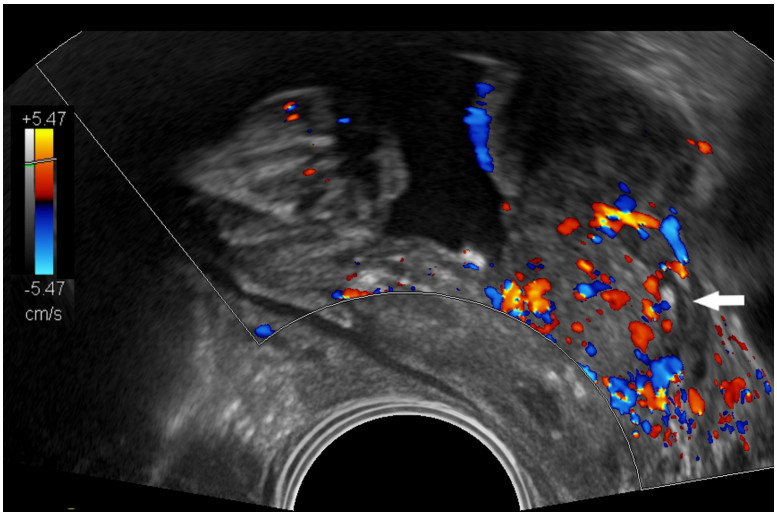

Contrast enhanced harmonic TRUS provides additional information on tissue perfusion (1). The examination is carried out with ultrasound contrast medium (SonoVue or regionally approved contrast media) using the low-MI ultrasound technique. The outer portions of the prostates show slower enhancement and lower contrast uptake on CH-TRUS compared to the central portions (4, 37). CH-TRUS provides information on the vascularization of focal lesions, especially in the outer zone, can detect hyperenhanced isoechoic lesions and can be used for targeted CH-TRUS guided biopsy (10). In combination with CE-TRUS and targeted biopsy, the rate of unnecessary biopsies could be reduced (15, 38). Furthermore, *3-D and 4-D TRUS* for spatial imaging and *fusion techniques* with MRI are possible (4, 45, 46). The MRI data sets can be fused with TRUS. In the TRUS, the findings that are suspicious in the MRI can then be specifically biopsied (4). A complex documentation for the mp TRUS is shown here in Figure 26. Focal findings detected in mpTRUS can then be targeted for mpTRUS guided biopsy [Figure 27].

Figure 26 **Illustrated is a complex multiparametric transrectal ultrasound scan (mpTRUS) of the prostate. The prostate is imaged via the rectum in B-mode TRUS. The prostate has a smooth border. Multiple calcifications are seen in the central parts. The peripheral zone is hyperechoic. Laterally there is a hyperechoic parenchymal change (a). The seminal vesicles present as polycyclic hypoechoic structures (b). The (strain) elastography in TRUS shows an intermediate image in the older patient, which alone is not helpful (c). Color Doppler imaging TRUS shows small vessels in the marginal area. Irregular hypovascularized structures are not delineated (d). In contrast enhanced harmonic TRUS, the central parts of the prostate are more enhancing than the periphery (e).**

a

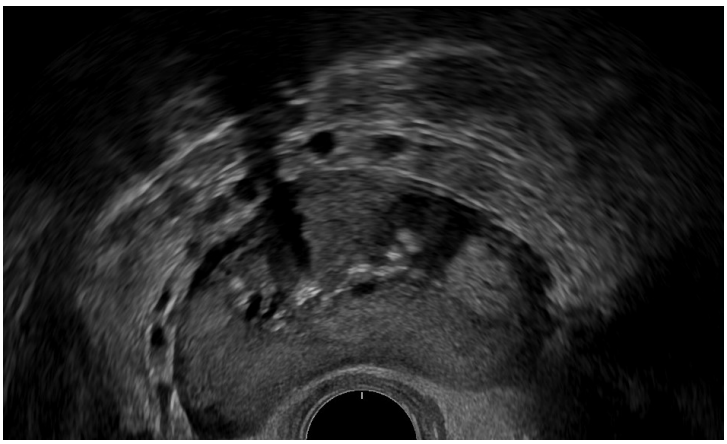

b

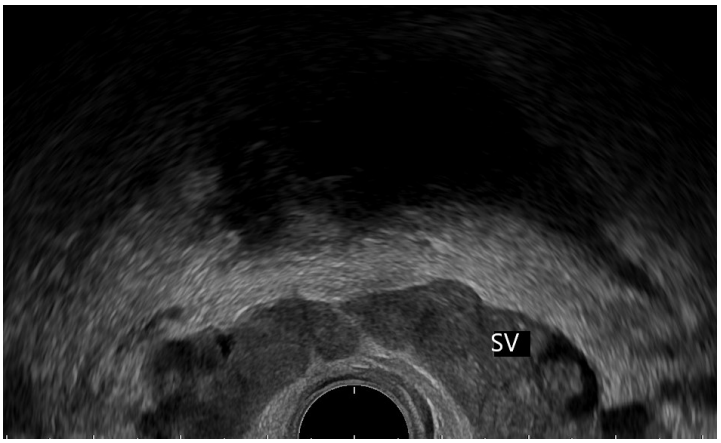

c

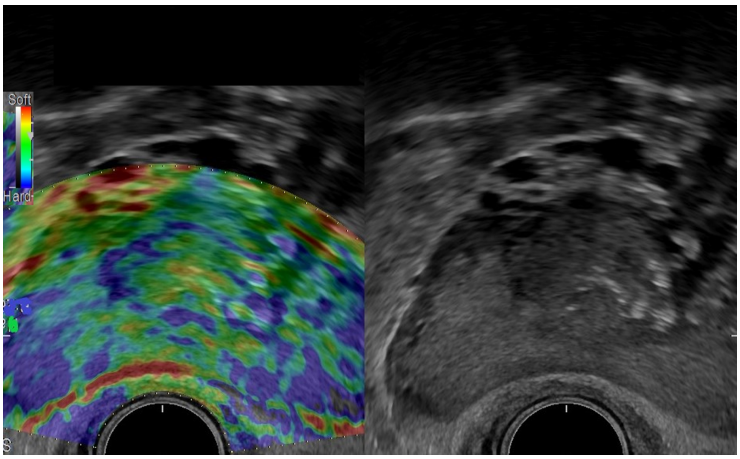

d

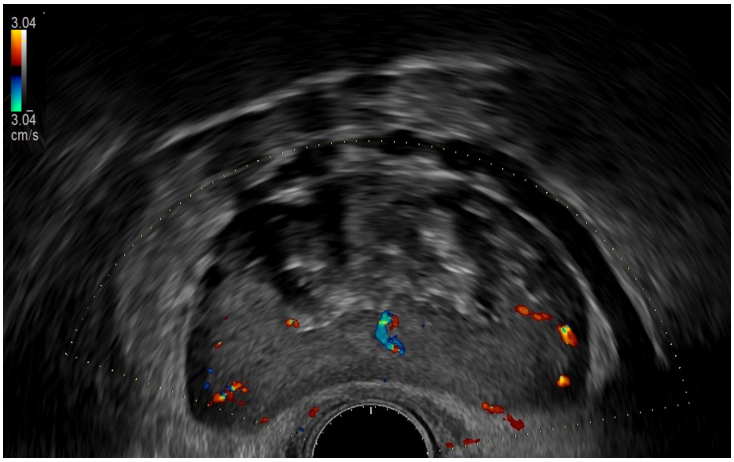

e

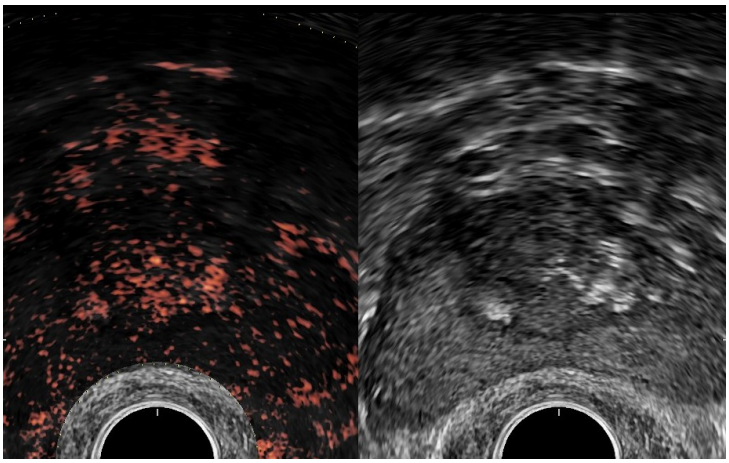

Figure 27 Mp-TRUS targeted biopsy of a B-mode hypoechoic (left image, white arrow) and elastographic (right image, white arrow) stiffer carcinoma. The yellow arrow demonstrates the biopsy needle.

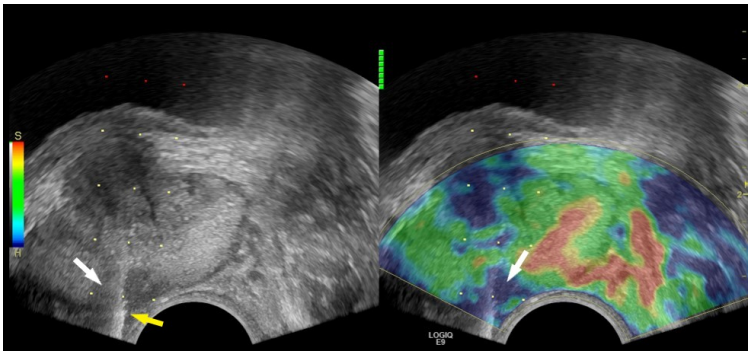

Multiparametric (mp) MRI

Multiparametric MRI is currently the gold standard for the investigation of prostatic lesions. Three sequences are studied in prostate MRI: T2-weighted imaging (T2- WI), dynamic contrast enhancement (DCE-MRI) and diffusion-weighted imaging (DWI-MRI (1). Tissue structure, cell density and tissue perfusion are assessed (1). The combination of T2-WI with at least two functional techniques (DCE-GRE, DWI) is defined to as *multiparametric MRI (mpMRI)*. The anatomical sequence (T2-WI) is used for the detection of tumor-specific focal lesions. The functional techniques then provide information on the blood flow and cell density of the lesion (10). Risk stratification of MRI findings is done by trained radiologists using the PI-RADS classification of the European Society of Urogenital Radiology (ESUR) and American College of Radiology (ACR). A score of 1 - 5 is assigned 1 = the presence of a clinically significant carcinoma is highly unlikely and 5 = the presence of a clinically significant carcinoma is highly probable. (47-49). All MRI guided biopsies have in common that they detect more significant carcinomas and fewer insignificant carcinomas. They require fewer punch biopsies for tumor detection. They are histologically closer to the RPE (radical prostatectomy) specimen. So they have a higher detection rate for clinically significant carcinomas.

Two methods have been developed in which ultrasound and mpMRI can be combined to perform prostate biopsy: cognitive biopsy and fusion biopsy. In the *cognitive* biopsy, the areas that were previously detected in the MRI and whose localization is precisely described are

biopsied in the TRUS. In the *fusion* biopsy, the MRI images are imported into the US device and fused with the B-TRUS mode [Figure 28] (10).

Figure 28 Technical fusion biopsy of a 2 mm carcinoma in the PZ base on the right (arrows): on the split ultrasound monitor, the live B-image appears on the left with the small lesion found only in fusion mode and on the right the T2 data set fed into the ultrasound device, which is moved simultaneously with the B-image. The patient is now under active surveillance.

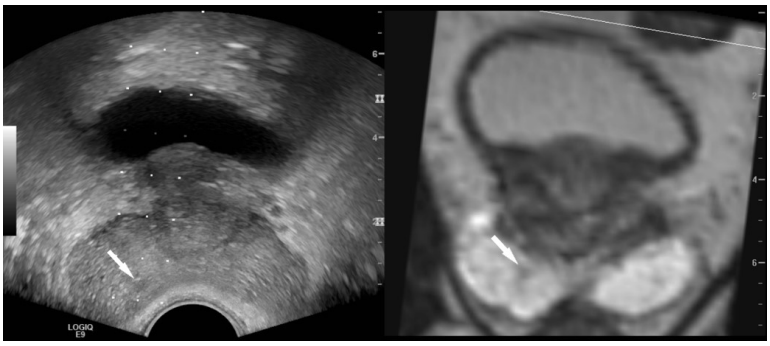

Using fusion biopsy, higher tumor detection rates were determined compared to systematic biopsy (50, 51). The mpTRUS and mpMRI data can also be merged and again led to an increased detection rate of significant prostate carcinomas in the targeted biopsy (52).

Importance of prostate ultrasound in clinical practice

The transabdominal examination of the prostate can be performed very easily. A favorable but not obligatory prerequisite for a better sound window is only a filled urinary bladder.
The most frequent indications are:

- LUTS, lower abdominal discomfort, micturition problems, clarification of urinary flow disorders, urinary tract infections, urinary catheter complications and increased renal retention parameters.
- Transabdominal US is not suitable for the detection of prostate carcinoma.

- TUS can be used to determine the size and volume of the prostate. Contour and echogenicity can be assessed, surrounding organs such as urinary bladder, seminal vesicles and regional lymph nodes.
- Focal lesions can be detected, but TUS is inferior to TRUS and MRI in the fine assessment of the parenchyma.

The fine assessment of the parenchyma with detection and differential diagnostic evaluation is subject to mpTRUS and mpMRI.

References

1. Pallwein-Prettner L, Aigner F: Techniken der Bildgebung in: Aigner F, Pallwein-Prettner L, Salomon G, Horninger W: Prostata. Multimodale Bildgebung. Ed.: 2nd ed: Breitenseher Publisher, 2018.
2. McNeal JE. The prostate and prostatic urethra: a morphologic synthesis. J Urol 1972;107:1008-1016.
3. Wasserman NF. Benign prostatic hyperplasia: a review and ultrasound classification. Radiol Clin North Am 2006;44:689-710, viii.
4. Steinkohl F, Luger A, Bektic J, Aigner F. [Ultrasonography of the prostate gland : From B-image through multiparametric ultrasound to targeted biopsy]. Radiologe 2017;57:615-620.
5. Chatterjee A, Thomas S, Oto A. Prostate MR: pitfalls and benign lesions. Abdom Radiol (NY) 2020;45:2154-2164.
6. Loch AC, Bannowsky A, Baeurle L, Grabski B, Konig B, Flier G, Schmitz-Krause O, et al. Technical and anatomical essentials for transrectal ultrasound of the prostate. World J Urol 2007;25:361-366.
7. Cao N, Lu Q, Si J, Wang X, Ni J, Chen L, Gu B, et al. The Characteristics of the Transitional Zone in Prostate Growth With Age. Urology 2017;105:136-140.
8. Kitzing YX, Prando A, Varol C, Karczmar GS, Maclean F, Oto A. Benign Conditions That Mimic Prostate Carcinoma: MR Imaging Features with Histopathologic Correlation. Radiographics 2016;36:162-175.
9. Tyloch JF, Wieczorek AP. The standards of an ultrasound examination of the prostate gland. Part 1. J Ultrason 2016;16:378-390.
10. Crisan N, Andras I, Radu C, Andras D, Coman RT, Tucan P, Pisla D, et al. Prostate ultrasound: back in business! Med Ultrason 2017;19:423-429.
11. Kim SH, Kim SH. Correlations between the various methods of estimating prostate volume: transabdominal, transrectal, and three-dimensional US. Korean J Radiol 2008;9:134-139.
12. Huang Foen Chung JW, de Vries SH, Raaijmakers R, Postma R, Bosch JL, van Mastrigt R. Prostate volume ultrasonography: the influence of transabdominal versus transrectal approach, device type and operator. Eur Urol 2004;46:352-356.

13. Ozden E, Gogus C, Kilic O, Yaman O, Ozdiler E. Analysis of suprapubic and transrectal measurements in assessment of prostate dimensions and volume: is transrectal ultrasonography really necessary for prostate measurements? Urol J 2009;6:208-213.
14. Aprikian S, Luz M, Brimo F, Scarlata E, Hamel L, Cury FL, Tanguay S, et al. Improving ultrasound-based prostate volume estimation. BMC Urol 2019;19:68.
15. Mitterberger M, Horninger W, Aigner F, Pinggera GM, Steppan I, Rehder P, Frauscher F. Ultrasound of the prostate. Cancer Imaging 2010;10:40-48.
16. Zhang SJ, Qian HN, Zhao Y, Sun K, Wang HQ, Liang GQ, Li FH, et al. Relationship between age and prostate size. Asian J Androl 2013;15:116-120.
17. Eri LM, Thomassen H, Brennhovd B, Haheim LL. Accuracy and repeatability of prostate volume measurements by transrectal ultrasound. Prostate Cancer Prostatic Dis 2002;5:273-278.
18. Qian S, Zhang S, Xia W, Xu D, Qi J, Shen H, Wu Y. Correlation of prostatic morphological parameters and clinical progression in aging Chinese men with benign prostatic hyperplasia: Results from a cross-sectional study. Prostate 2021;81:478-486.
19. Randall A HFJ. Surgical anatomy of the prostatic lobes. New York: Springer Verlag, 1983: 672-676.
20. Galosi AB, Montironi R, Fabiani A, Lacetera V, Galle G, Muzzonigro G. Cystic lesions of the prostate gland: an ultrasound classification with pathological correlation. J Urol 2009;181:647-657.
21. Klimas R, Bennett B, Gardner WA, Jr. Prostatic calculi: a review. Prostate 1985;7:91-96.
22. Sfanos KS, Wilson BA, De Marzo AM, Isaacs WB. Acute inflammatory proteins constitute the organic matrix of prostatic corpora amylacea and calculi in men with prostate cancer. Proc Natl Acad Sci U S A 2009;106:3443-3448.
23. Kapogiannis F, Fasoulakis K, Fragkoulis C, Aggelopoulos A, Fasoulakis C. Total Osseous Calcification of the Prostate Gland. Cureus 2020;12:e9239.
24. Wang H, Ma M, Qin F, Yuan J. The influence of prostatic calculi on lower urinary tract symptoms and sexual dysfunction: a narrative review. Transl Androl Urol 2021;10:929-938.
25. Hyun JS. Clinical Significance of Prostatic Calculi: A Review. World J Mens Health 2018;36:15-21.
26. Peeling WB, Griffiths GJ. Imaging of the prostate by ultrasound. The Journal of urology 1984;132 2:217-224.
27. Harada K, Igari D, Tanahashi Y. Gray scale transrectal ultransonography of the prostate. J Clin Ultrasound 1979;7:45-49.
28. Vilches J, López A, De Palacio L, Muñoz C, Gómez J. SEM and X-ray microanalysis of human prostatic calculi. The Journal of urology 1982;127 2:371-373.
29. Cao JJ, Huang W, Wu HS, Cao M, Zhang Y, Jin XD. Prostatic Calculi: Do They Matter? Sex Med Rev 2018;6:482-491.
30. Smolski M, Turo R, Whiteside S, Bromage S, Collins GN. Prevalence of prostatic calcification subtypes and association with prostate cancer. Urology 2015;85:178-181.
31. Shakur A, Hames K, O'Shea A, Harisinghani MG. Prostatitis: imaging appearances and diagnostic considerations. Clin Radiol 2021;76:416-426.
32. Maurice MJ, Zhu H. Sarcoidosis of the prostate. J Urol 2013;190:711-712.
33. Furusato B, Koff S, McLeod DG, Sesterhenn IA. Sarcoidosis of the prostate. J Clin Pathol 2007;60:325-326.
34. Block NL, Kava BR. Genitourinary sarcoidosis: An essential review for the practicing clinician. Indian J Urol 2017;33:6-12.

35. Yoshimura Y, Takeda S, Ieki Y, Takazakura E, Koizumi H, Takagawa K. IgG4-associated prostatitis complicating autoimmune pancreatitis. Intern Med 2006;45:897-901.
36. Lohr JM, Beuers U, Vujasinovic M, Alvaro D, Frokjaer JB, Buttgereit F, Capurso G, et al. European Guideline on IgG4-related digestive disease - UEG and SGF evidence-based recommendations. United European Gastroenterol J 2020;8:637-666.
37. Trabulsi EJ, Sackett D, Gomella LG, Halpern EJ. Enhanced transrectal ultrasound modalities in the diagnosis of prostate cancer. Urology 2010;76:1025-1033.
38. Zhao HW, Li J, Cao JZ, Lin J, Wang Z, Lv JY, Wei JH, et al. Contrast-enhanced transrectal ultrasound can reduce collection of unnecessary biopsies when diagnosing prostate cancer and is predictive of biochemical recurrence following a radical prostatectomy in patients with localized prostate cancer. BMC Urol 2020;20:100.
39. Mottet N, Bellmunt J, Bolla M, Briers E, Cumberbatch MG, De Santis M, Fossati N, et al. EAU-ESTRO-SIOG Guidelines on Prostate Cancer. Part 1: Screening, Diagnosis, and Local Treatment with Curative Intent. Eur Urol 2017;71:618-629.
40. Mottet N, van den Bergh RCN, Briers E, Van den Broeck T, Cumberbatch MG, De Santis M, Fanti S, et al. EAU-EANM-ESTRO-ESUR-SIOG Guidelines on Prostate Cancer-2020 Update. Part 1: Screening, Diagnosis, and Local Treatment with Curative Intent. Eur Urol 2021;79:243-262.
41. Serefoglu EC, Altinova S, Ugras NS, Akincioglu E, Asil E, Balbay MD. How reliable is 12-core prostate biopsy procedure in the detection of prostate cancer? Can Urol Assoc J 2013;7:E293-298.
42. Peltier A, Aoun F, El-Khoury F, Hawaux E, Limani K, Narahari K, Sirtaine N, et al. 3D versus 2D Systematic Transrectal Ultrasound-Guided Prostate Biopsy: Higher Cancer Detection Rate in Clinical Practice. Prostate Cancer 2013;2013:783243.
43. Mohler JL, Antonarakis ES, Armstrong AJ, D'Amico AV, Davis BJ, Dorff T, Eastham JA, et al. Prostate Cancer, Version 2.2019, NCCN Clinical Practice Guidelines in Oncology. J Natl Compr Canc Netw 2019;17:479-505.
44. Tyloch DJ, Tyloch JF, Adamowicz J, Juszczak K, Ostrowski A, Warsinski P, Wilamowski J, et al. Elastography in prostate gland imaging and prostate cancer detection. Med Ultrason 2018;20:515-523.
45. Uno H, Taniguchi T, Seike K, Kato D, Takai M, Iinuma K, Horie K, et al. The accuracy of prostate cancer diagnosis in biopsy-naive patients using combined magnetic resonance imaging and transrectal ultrasound fusion-targeted prostate biopsy. Transl Androl Urol 2021;10:2982-2989.
46. Postema AW, Scheltema MJ, Mannaerts CK, Van Sloun RJ, Idzenga T, Mischi M, Engelbrecht MR, et al. The prostate cancer detection rates of CEUS-targeted versus MRI-targeted versus systematic TRUS-guided biopsies in biopsy-naive men: a prospective, comparative clinical trial using the same patients. BMC Urol 2017;17:27.
47. Turkbey B, Rosenkrantz AB, Haider MA, Padhani AR, Villeirs G, Macura KJ, Tempany CM, et al. Prostate Imaging Reporting and Data System Version 2.1: 2019 Update of Prostate Imaging Reporting and Data System Version 2. Eur Urol 2019;76:340-351.
48. Dutruel SP, Jeph S, Margolis DJA, Wehrli N. PI-RADS: what is new and how to use it. Abdom Radiol (NY) 2020;45:3951-3960.
49. Linhares Moreira AS, De Visschere P, Van Praet C, Villeirs G. How does PI-RADS v2.1 impact patient classification? A head-to-head comparison between PI-RADS v2.0 and v2.1. Acta Radiol 2021;62:839-847.

50. Borghesi M, Bianchi L, Barbaresi U, Vagnoni V, Corcioni B, Gaudiano C, Fiorentino M, et al. Diagnostic performance of MRI/TRUS fusion-guided biopsies vs. systematic prostate biopsies in biopsy-naive, previous negative biopsy patients and men undergoing active surveillance. Minerva Urol Nephrol 2021;73:357-366.
51. Bass EJ, Pantovic A, Connor MJ, Loeb S, Rastinehad AR, Winkler M, Gabe R, et al. Diagnostic accuracy of magnetic resonance imaging targeted biopsy techniques compared to transrectal ultrasound guided biopsy of the prostate: a systematic review and meta-analysis. Prostate Cancer Prostatic Dis 2022;25:174-179.
52. Zhang X, Hong H, Liang D. The combined value of mpUS and mpMRI-TRUS fusion for the diagnosis of clinically significant prostate cancer. Cancer Imaging 2022;22:60.